Biological Engineering Conference - CHEMPOR 2008
Braga, Portugal, September 4-6, 2008
E.C. Ferreira and M. Mota (Eds.)

Extending Kozeny-Carman permeability model to highly porous media

Manuel Mota*, Alexander Yelshin
IBB – Institute for Biotechnology and Bioengineering, Centre of Biological Engineering, University of Minho, Campus de Gualtar, 4710–057 Braga, Portugal.

Keywords: Permeability, Porosity, Tortuosity, Shape factor, Model
Topic: Advancing the chemical and biological engineering fundamentals.

Abstract

Anomalous normalised permeability as a ratio of permeability to square of particle size for snow, diatomite, kieselgel was considered using Kozeny-Carman model and tortuosity factor defined as the square of average tortuosity pathway. Since the Kozeny-Carman model is based on the geometrical models of a capillary tube, the model adopted for high porous media with shaped particles (often with fractal properties) becomes complex. To show how the problem of permeability may be complex, two types of particles are analysed in porous media: snowflakes and diatomite and kieselguhrs. Snowflakes are typical fractal particles, whereas diatomite and kieselguhr can form pores with fractal tortuosity. Based on theoretical investigation a model including fractal measurements for void and solid phases and dependence of tortuosity on packing porosity is proposed. The obtained results show that within the developed model we can describe a wide range of porous media with different fractality and tortuosity. Based on presented numerous examples it was concluded that further experimental investigation should be useful to improve the model and validate the application range.

1. Introduction

Highly porous media play a significant role in many practical applications including nanotechnology, biomedicine, fuel cells, catalysis etc. However, the interpretation of experimental permeability data is difficult whenever the particle shape or particle arrangement becomes significantly different of conventional granular packing.

In this case conventional Kozeny-Carman model (1) does not satisfy experimental conditions

$$k = \frac{\varepsilon^3}{K_0 \tau^2 (1-\varepsilon)^2 S^2} = \frac{d^2 \varepsilon^3}{36 K_0 \tau^2 (1-\varepsilon)^2} = \frac{d^2 \varepsilon^3}{72 \tau^2 (1-\varepsilon)^2} \quad (1)$$

where k is the permeability, 1/m; S is the specific surface area based on the solid volume; $d = 6/S$ is the equivalent spherical particle size; ε is the porosity; $K_0 \tau^2$ includes tortuosity τ (ratio of average pathway to the porous medium thickness) and K_0 - a coefficient dependent on the pore cross-section shape (for cylindrical pores K_0 = 2). In particular cases model (1) may be used in the form

$$k = (d^2 \varepsilon^3)/[180(1-\varepsilon)^2] \quad (1a)$$

As Kozeny-Carman model is based on the geometrical models of a capillary tube, then the model adopted for high porous media with shaped particles (often with fractal properties) becomes complex (see Figs. 1 - 2).

In some cases porous media with fractal wall surface do not have a fractal tortuosity of pore channels, as in Fig. 1 (a-b) or, in contrary, display a fractal dimension dependent

* Corresponding author. Tel + 351-25360-1191. E-mail: MMota@reitoria.uminho.pt

on a channel topology, as in Fig. 1 (c-e). In theses examples two fractal curves with different fractal dimension were used to built the pore channels: (a) von Koch snowflake curve, fractal dimension 1.26, has 4 levels of structure, each level with tortuosity τ_i = 4/3, and the overall tortuosity of the curve is $\tau \approx$ 3.16, Fig. 1a; the (b) curve has fractal dimension 1.5, 3 levels of structure, each level with a tortuosity τ_i = 2, and overall tortuosity of the curve is τ = 8, Fig. 1b. The case in Fig. 1 (a-b) corresponds to the symmetrical pore channel with fractal perimeter (contour) where a centreline geometrical tortuosity is equal to 1.

In the case of non-symmetrical pore channels, Fig. 1 (c) and (d), built by fractal curves of types (a) and (b), they have a centreline tortuosity of τ = 1.97 and 2.62 with a fractal dimension of 1.01 and 1.03. In turn, in case (e), tortuosity is much higher, τ = 8, and the fractal dimension of pore channel walls is 1.5. Moreover, the porous medium fractal dimension is dependent on porosity and on the particle shape.

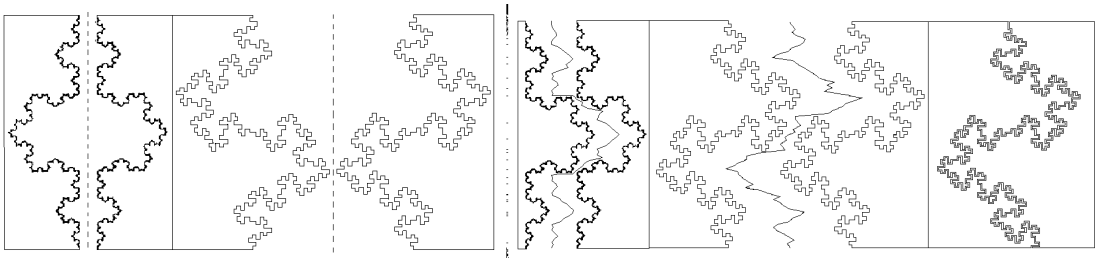

Figure 1. Two symmetrical pore channels built by fractal curves (See text) having the average geometrical tortuosity τ = 1.0, case (a) and (b). Non-symmetrical pore channels built by fractal curves, cases (c-d).

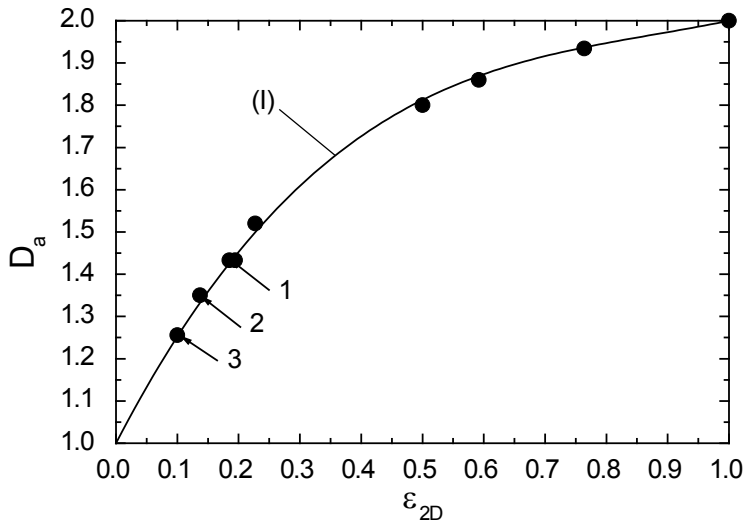

Figure 2. Fractal dimension D_a vs. ε_{2D} for regular packing of discs: 1 – square packing; 2 – hexagonal packing; 3 – discs square arrangement of two sizes (space between large size square packing filled by inscribed discs). I – correlation function.

Porous media porosity is one of the most important characteristics involved in all models of mass and heat transfer. Dependence of the 2D porous media fractal properties on porosity (ε_{2D}) is shown in Fig. 2, where a disc type porous structures are presented. Increasing porous media complexity (the structure deviates from uniformity)

renders the topological properties of the system (fractal dimension) dominant.

As can be seen, porosity and tortuosity are interrelated and both connected with fractal properties of porous media and properties interplay gives different results. For instance, a carbon felt (*Le Carbone Lorraine*, RVC 4002) for electrodes has the porosity 0.98 and tortuosity 5 – 6, (González-Garcia et al., 1999); α-alumina catalyst pellet, ε = 0.68, average tortuosity 4.0,(Dogu et al. ,1989); iron-based Fischer-Tropsch catalyst, ε = 0.628, tortuosity ~ 6.0, (Eaton et al. , 1995); mica (powdered) and vermiculite at porosity 0.85 – 0.9 have tortuosity over 2.0, (Currie ,1960).

2. Theoretical background

To show how the problem may be complex, two types of particles are considered below: snowflake and diatomite/kieselguhr.

Jordan et al. (1999) summarised and analysed published and own experimental data on snow permeability by using Kozeny-Carman model in the form (1a) and an approach of the form

$$k = 0.077 d^2 \exp(-0.0078 \rho_i (1-\varepsilon)) \qquad (2)$$

where ρ_i = 917 is ice density, kg/m^3.

Normalised experimental snow permeability k/d^2 together with models (1a) and (2) are shown in Fig. 3, where some data for low-density snow are below theoretical predictions for a granular bed (curve 1) as well as for a model (2), curve 2.

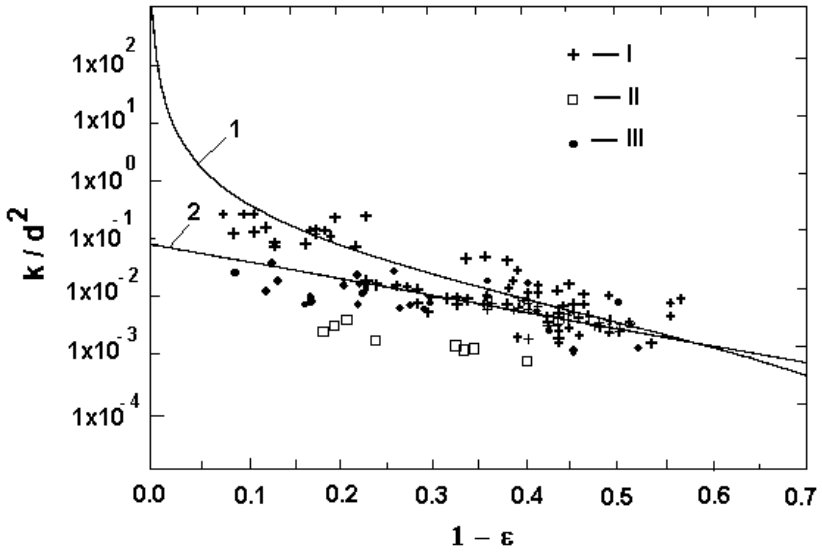

Figure 3. Reduced permeability k/d^2 vs. ice fraction $\phi = 1-\varepsilon$ as presented by Jordan (1999) in fig. 7. I – Shimizu, Ishido and Shimizu data; II – Sommerfeild and Rocchio data; III - Jordan data. 1 – granular bed model, equation (1a); 2 – approach, equation (2).

According to snow classification by solid fraction and permeability (Jordan , 1999), the main part of snow samples which does not fit to the above mentioned models belong to wind-packed (dense) and new snow (low density) which leads to consider particle shape as an important parameter of the permeability behaviour. However, in (2) we can speculate that $(1-\varepsilon)$ is accounted for in fractal properties as well.

For non-spherical particle the model (1) may be partially corrected by introducing a sphericity factor Φ of a particle as the ratio of the surface area of a sphere S (with the same volume as the given particle) to the surface area of the particle S_p, $\Phi = S/S_p$, hence, $d_p = 6/S_p = 6\Phi/S = \Phi d$. In this case, fractal behaviour may affect all or part

of variables (Xu and Yu, 2008): pore space (ε), solid ($1-\varepsilon$) or ratio $\varepsilon/(1-\varepsilon)$, and tortuosity ($\tau$).

In general, the tortuosity depends on porosity and may be presented in the form $\tau = a/\varepsilon^n$ ($n \geq 0$; $a \geq 1$, conventionally a = 1). By substituting τ and Φ in (1) and introducing the normalised permeability we have the following $k/d^2 = (\Phi^2/K_0)[\varepsilon^3/(36\cdot(a/\varepsilon^n)^2(1-\varepsilon)^2)]$. The value of K_0 depends on a pore cross-section configuration that, in turn, reflects the particles shape. Since the exact relations between Φ, K_0 and ε are unknown, complex $\Phi^2/(K_0 a^2)$ can be considered as the fitting coefficient $1/A$.

If we assume that in porous media structure particles are generated from sub-units of smallest scale, as shown in Fig. 4, then external and internal factors may yield substantial particle transformation. In the case of snow, primary snowflake melting results in porous media compaction and in structural degradation, with loss of fractal properties and an approach to granular packing.

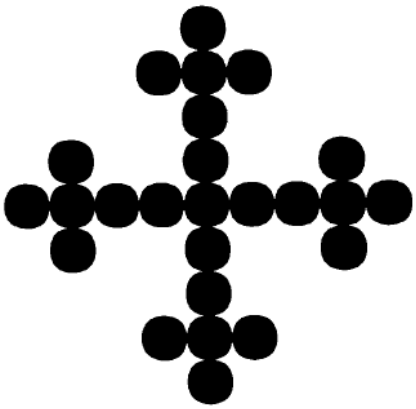

Figure 4. Simplified representation of a complex primary particle structure build by sub-units.

Structural properties based upon fractal analysis must be introduced in normalised permeability under the form of ΔD and $\Delta_1 D\cdot\varphi(\varepsilon)$ as fractal measures for void and solid phases, where $0 \leq \Delta D \leq 1$, $0 \leq \Delta_1 D \leq 1$, and $\varphi(\varepsilon)$ is a function accounting for deviation of porous media from granular packing. Finally, dependence of normalised permeability on porosity becomes

$$k/d^2 = \frac{\varepsilon^{3\Delta D}}{36A(1/\varepsilon^n)^2(1-\varepsilon)^{2\Delta_1 D\cdot\varphi(\varepsilon)}} = \frac{\varepsilon^{3\Delta D+2n}}{36A(1-\varepsilon)^{2\Delta_1 D\cdot\varphi(\varepsilon)}} \quad (3)$$

3. Discussion

Two types of particles are presented in Fig. 5: snowflakes (shaded area occupied by data of Jordan et al. (1999)), diatomite (I), from Yoon et al. (1992) and kieselguhrs (II), Mota et al. (2000, 2003). Snow represents fractal particles, whereas diatomite and kieselguhr can form pores with a significant fractal tortuosity.

Application of relation (1a) and model (2) as proposed for the snow layer (Fig. 5), gives rise to curves 1 and 2, respectively. Ignoring dependence of τ on ε does not allow covering the whole region of experimental data. Conventional model (1) has as upper limit τ = 1.0 and curve 1′ is far from the experimental bounds.

The model (3) was accepted and deviation from granular packing $\varphi(\varepsilon)$ was assumed

to be $\varphi(\varepsilon) = 1 + \varepsilon_0 - \varepsilon$. The function $\varphi(\varepsilon)$ = 1 when $\varepsilon = \varepsilon_0$ where ε_0 has a value in the range 0.3 – 0.45 and is defined as a fitting parameter.

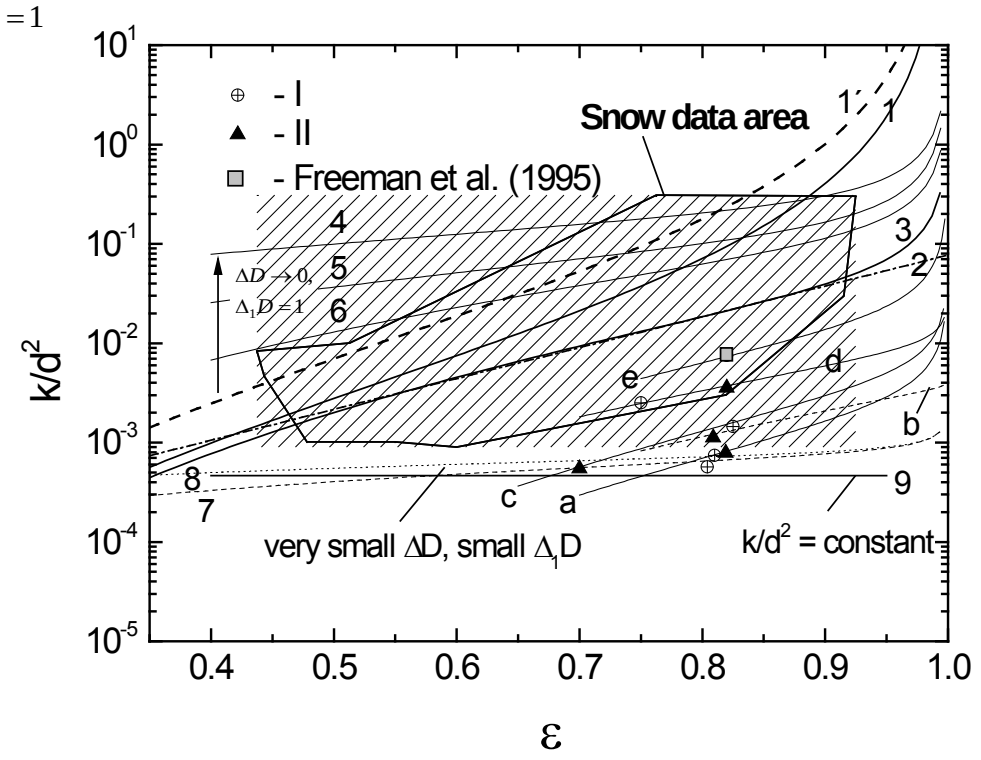

Fig. 5. Normalised permeability k/d^2 vs. porous media porosity. Shaded area is occupied by snow data of Jordan et al. (1999). 1 – equation (1a); 1´ – case (1) when τ = 1; 2 – relation (2); 3 – fitting relation (2) by model (3). Curves a – e are fitting data of mineral porous media: a - Kieselguhr fine; b – Kieselgel; c - Radiolite 600; d - Dialite UND; e – Kieselguhr. For curves 4 – 9 see the text.

Table 1. Coefficients of model (3) for curves presented in Figure 5

Curve	ΔD	$\Delta_1 D$	n	ε_0	A
4	0	1	0	0.42	1
5	0.1	1	0.1	0.45	2
6	0.3	1	0.5	0.4	2
3	0.69	1	0.6	0.4	5
Granular packing	1	1	0.4-0.5	$\varepsilon_0 = \varepsilon$	2
e	1	1	0.5	0.35	10.54
d	1	0.35	0.5	0.35	6.36
b	1	0.05	1	0.3	8.64
c	1	0.78	1	0.35	27.8
a	1	0.8	1	0.38	58.4
7	0.05	0.25	0.25	0.4	60
8	0.05	0.25	0.025	0.4	60
9	0	0	0	--	60

The obtained results show that within model (3) we can describe a wide range of porous media. In particular for snow, correlation (2), curve 2, is well fitted by model 3 (curve 3) with the following parameters: ΔD = 0.69, n = 0.6, A = 5, and ε_0 = 0.4. For new snow, in particular, a tendency (Fig. 5, arrow) to increase the permeability was found, when

$\Delta D \to 0$ and $\Delta_1 D = 1$. Curve 4 corresponds to the case $\Delta D = 0$, $\tau = 1$, when A = 1: $k/d^2 = 1/[36(1-\varepsilon)^{2(1.42-\varepsilon)}]$. Moreover, model (3) at $\varepsilon \to$ 1 gives $k/d^2 \to \infty$, whereas correlation (2) gives finite normalised permeability value. Examples of fitting data of mineral porous media by (3) are given by curves a – e and are also presented in Table 1: a - Kieselguhr fine; b – Kieselgel; c - Radiolite 600; d - Dialite UND; e – Kieselguhr.

Dependences 7 – 9 are hypothetic and simulate cases of very small ΔD. With decreasing ΔD and $\Delta_1 D$ we observe insignificant linear changes in k/d^2 and in limited case of ΔD and $\Delta_1 D$ equal zero dependence (3) becomes constant $k/d^2 = 1/(36A)$, as seen in Fig 5, bottom, curve 9. Even in the hypothetic case of A = 60 and a = 1 for Φ = 0.5 we have K_0 = 15. Assuming a = 1.5, K_0 becomes 6.7 and at a = 2 K_0 = 3.75. Formally, this situation is related with the degradation of porous media structure when tortuosity weakly depends on porosity, which is typical for non-granular porous media. For instance, when porous media contain homogeneous pores similar in length the porosity totally depends on number of pores on unit area of porous medium. Fractality behaviour of such systems is not enough investigated.

Model (3) allows simulating and predicting permeability or other parameters when experimental data are scarce.

4. Conclusion

Obtained results form the modified Kozeny-Carman model show that application of the fractal approach to the porous media void space as well as to solid phase enables to extend the model to highly porous media. The obtained results show that within the developed model we can describe a wide range of porous media with different fractality and tortuosity. In spite of the numerous examples presented, further experimental investigation will be useful to improve the model and validate its application range.

References

González-Garcia, J., Bonete, P.B., Expósito, E., Montiel, V., et al. (1999). *J. Mater. Chem.*, 9, 419-426.

Dogu, G., Pekediz, A., Dogu, T. (1989). *AIChE Journal*. 35, 1370-1375.

Eaton, A., Bukur, D.B., Akgerman, A. (1995). *J. Chem. Eng. Data.* 40, 1293-1297.

Currie, J.A. (1960). *Brit. J. Appl. Phys.* 11, 318-324.

Jordan, R.E., Hardy, J.P., Perron, F.E., Fisk, Jr.J., et al. (1999). *Hydrological Processes*, 13, 1733-1753.

Xu, P., Yu, B. (2008). *Advances in Water Resources*, 31, 74–81.

Yoon, S.-H., Murase, T., Iritani, E. (1992). *Int. Chem. Eng.*, 32, 172-180.

Mota, M., Teixeira, J. A., Bowen, R., Yelshin, A. (2000). *Proc. 8-th World Filtration Congress, 3-7 April 2000*, Volume 1, Filtration Society, Brighton, UK, 57-60.

Mota, M., Teixeira, J. A., Bowen, R., Yelshin, A. (2003). *Minerals Engineering*. 16, 135-144.

Freeman, G.J., Mckechnie, M.T., Smedley, S.M., Hammond, R.V., et al. (1995). *Trans. IChemE*, 73, 157-164.